Numerical Analysis OF PCM Within a Square Enclosure Having Different Wall Heating Conditions

Pallab Bhattacharjee, Sujit Nath, and Dipankar Bhanja

Abstract In the present study, the melting of phase change material (PCM) in a square enclosure with different wall heating conditions has been studied numerically. It has been found that at the early stage of melting, PCM melts faster in case of bottom wall heating. Melting for sidewall heating transcends the melting of bottom wall heating in a later stage. However, the increase of solid–liquid interface length leads to higher convective heat transfer for side wall heating in later part of melting. On the other hand, isothermal heating from the upper wall results in thermal stratification of PCM layers which leads to no convection. So, the melting time is quite large for this case.

Keywords PCM · Thermal energy reservoir · Melt fraction

Nomenclature

c_p	Specific heat at constant pressure (KJ/kgK)
g	Gravitational acceleration
k	Thermal conductivity
T	Temperature (K)
H	Length of square arm (m)
α	Coefficient of thermal diffusivity (m^2/s)
β	Coefficient of thermal expansion (1/K)
μ	Dynamic viscosity (Pa-s)
ρ	Density (Kg/m^3)

P. Bhattacharjee (✉) · S. Nath · D. Bhanja
Mechanical Engineering, National Institute of Technology, Silchar, Assam, Silchar 788010, Assam, India
e-mail: bhattacharjeepallab27@gmail.com

477

Subscripts

l   liquid
m   melting
w   wall
s   solid
avg   average

1   Introduction

High amount of energy can be stored during phase change process of phase change material with a negligible change in temperature. Thus, PCM has the potential to be used as energy reservoir in thermal systems, refrigeration, and air conditioning unit. But the challenge associated with PCM is very low thermal conductivity which results in slow charging and discharging. Researchers have used different techniques such as mixing high conductive nanoparticles with PCM, using different types of finned structures [2, 3], using metal matrix, incorporation of heat pipe, and using multiple PCM at a time [1].

Biwole et al. [2] studied the influence of fin size and distribution on solid–liquid phase change in a rectangular enclosure. They found that increasing the number of fin reduces the temperature of the plate and also accelerates melting process. Using thinner and longer fins also improves melting marginally. Ji et al. [3] explored the effect of fin placement at different inclination angles in a rectangular enclosure. Minimum melting time was obtained for 15º downward tilted fin. Upward tilted fin gives rise to uneven heating thus increasing the melting time. Kamkari et al. [1] have done both numerical and experimental study on inclined rectangular enclosures. It was found that for complete melting 0° and 45°, enclosures take 52 and 37% shorter time, respectively, in comparison with vertical enclosure. Asl et al. [4] had investigated the solid and porous fin in inclined rectangular enclosure. It has been predicted that porous fins are more effective with high Raleigh number and with highly conductive material. Ebadi et al. [5] did a numerical analysis and finally validated experimentally on melting of nano-PCM inside a cylindrical thermal energy reservoir (TES). In their work, the bio-based coconut oil PCM with dispersed copper oxide nanoparticles inside a cylindrical container is heated isothermally from lateral walls and from the top. Adding copper oxide nanoparticles improved the melting at later stage when dispersion of nanoparticle starts. Arena et al. [6] numerically analyzed a latent heat thermal energy storage system under partial load operating conditions. A substantial reduction in the duration of the TES (up to 50%) process against a small decrease in stored energy (up to 30%) has been noticed. Shokouhmand et al. [7] tried to apprehend the temperature field with melt front in a rectangular enclosure. They interpreted that the conduction is dominant at the beginning but convection is dominant in the later part of melting. The convection heat transfer in

the later stage also reduces due to thermal stratification. Dhar et al. [8] analyzed the remelting phenomenon of eutectic aqueous ammonium chloride solution in a top cooled rectangular cavity during solidification process. It has been observed that remelting occurs during the progress of solidification however it depends on cavity height as well as imposed temperature gradient.

In the present work, the effect of heating at different walls of a rectangular enclosure is studied to find out the best heating strategy for getting higher melting rate. For this, a numerical model is developed with specific heat capacity formulation by COMSOL Multiphysics 5.3. Lauric acid is taken as PCM and kept in a square enclosure which is heated isothermally from different sides like left wall, top wall, and bottom wall, respectively.

2 Description of Numerical Model

A 2D numerical model is built with finite element-based software COMSOL Multiphysics 5.3. The model consists of a square enclosure filled with lauric acid. An implicit time stepping scheme along with a parallel sparse direct solver (PARDISO) is used to solve the governing equations. The absolute tolerance for scaled residues of the variables is 10^{-2}. A total 1375 triangular and 232 quadratic mesh have been generated for the model. The results are independent with average element quality 0.815. The properties of lauric acid [2] are given in Table 1. The container is heated isothermally from different sides at 343 K wall temperature (T_w). The square container has a dimension of 0.06 m × 0.06 m. There is a thin aluminum plate of 0.002 m width at heating surface.

Governing equations

For the present PCM model, the following equations [6] have been used to simulate the charging and discharging process.

Continuity equation

$$\frac{\partial \rho}{\partial t} + \nabla.(\rho \vec{u}) = 0 \tag{1}$$

Table 1 Thermophysical properties of lauric acid

Property	Value	Property	Value
$c_{p,s}$	2180 J/(kg K)	ρ_s	940 kg/m^3
$c_{p'l}$	2390 J/(kg K)	ρ_l	885 kg/m^3
L	187,200 J/(kg K)	μ	8×10^{-3} kg/(m s)
k_s	0.16 W/(m k)	β	8×10^{-4} K^{-1}
k_l	0.14 W/(m k)	T_m	316.65 K

Momentum equation

$$\frac{\partial \rho \, \vec{u}}{\partial t} + \rho (\vec{u} \cdot \nabla) \, \vec{u} - \nabla \cdot [\mu (\nabla \vec{u} + (\nabla \vec{u})^T)] + \nabla p = \vec{F} \tag{2}$$

Energy equation

$$\rho c_p \frac{\partial T}{\partial t} + \rho c_p \, \vec{u} \, \nabla T = \nabla \cdot (k \nabla T) \tag{3}$$

where ρ is density, $\vec{u}$ is velocity vector, μ is dynamic viscosity, p is pressure, T is temperature, t is time, and $\vec{F}$ is the body force. For modeling the phase change process, Eq. (3) is modified using specific heat capacity formulation by Eq. (4) [6]. In the specific heat capacity formulation, the latent heat (L) term is added. The phase change process takes between $(T_m - \Delta T_m/2)$ to $(T_m + \Delta T_m/2)$ temperature. Here θ is defined as melt fraction, which is 0 for temperature less than $(T_m - \Delta T_m/2)$ and 1 for temperature more than $(T_m + \Delta T_m/2)$. The range of phase change temperature is taken $\Delta T_m = 2\ °C$.

$$c_p = \frac{1}{\rho} [(1 - \theta) \rho_{phase1} c_{p,\,phase1} + \theta \rho_{phase2} c_{p,\,phase2}] + L \frac{\delta \alpha}{\delta T} \tag{4}$$

The effective conductivity is calculated as [6]

$$k = (1 - \theta) k_{phase1} + \theta k_{phase2} \tag{5}$$

The effective density is evaluated as

$$\rho = (1 - \theta) \rho_{phase1} + \theta \rho_{phase2} \tag{6}$$

The mass fraction α is expressed as [6]:

$$\alpha = \begin{bmatrix} -\frac{1}{2} \left\{ T < T_m - \frac{\Delta T_m}{2} \right\} \\ \frac{1}{2} \frac{\theta \rho_{phase2} - (1 - \theta) \rho_{phase1}}{\rho} \left\{ T_m - \frac{\Delta T_m}{2} < T < T_m + \frac{\Delta T_m}{2} \right\} \\ \frac{1}{2} \left\{ T > T_m + \frac{\Delta T_m}{2} \right\} \end{bmatrix} \tag{7}$$

As the total PCM is treated as liquid always, the body force term of the Navier–Stokes equation is modified to calculate velocity of the PCM even if in solid state. One part of the body force as expressed in Eq. (8) is to cater buoyant force (F_b) which is responsible for natural convection, where Boussinesq approximation is used.

$$\vec{F}_b = g\rho_l\beta(T - T_m) \tag{8}$$

where ρ_l, β, g, and T_m are density of liquid PCM, thermal expansion coefficient, gravitational constant, and melting temperature, respectively. Along with this part of the body force, Carman–Kozeny equation [6] is also used to add one more volume force in the momentum equation as expressed in Eq. (9).

$$\vec{F}_v = -A(T)\vec{u} \tag{9}$$

$$A(T) = A_{\text{mush}}\frac{(1-\theta)^2}{(\theta^3 + \varepsilon)} \tag{10}$$

where the constants A_{mush} and ε are having the values of 10^5 and 10^{-3}, respectively [6]. The term ε is used to avoid division by 0 when θ is equal to zero. The value of $A(T)$ is very high in solid state of PCM, when melt fraction tends to zero [2]. But its value tends to 0 for liquid state of PCM. This volume force term actually makes the velocity approximately 0 in solid PCM and to a finite value in liquid region for solving the momentum equation. The viscosity as expressed in Eq. (11) is also modified for temperature less than $T_m - \frac{\Delta T_m}{2}$.

$$\mu(T) = \mu_{\text{liquid}}(1 + A(T)) \tag{11}$$

   Nusselt number gives a measure of approximate heat transfer from the heating surface. In the present study, the average Nusselt number for the side wall and upper/lower wall is expressed as Eqs. (12) and (13), respectively [9].

$$Nu_{\text{avg}} = -\frac{1}{T_h - T_m}\int_0^H \left(\frac{\partial T}{\partial x}\right)_{x=x_{\text{wall}}} dy \tag{12}$$

$$Nu_{avg} = -\frac{1}{T_h - T_m}\int_0^H \left(\frac{\partial T}{\partial y}\right)_{y=y_{wall}} dx \tag{13}$$

2.1 Boundary and Initial Condition

No-slip boundary condition at all solid walls, i.e., $u = v = 0$; isothermal boundary condition ($T = T_w$) at the heated wall; rest of the walls are insulated, i.e., $\frac{\partial T}{\partial n} = 0$ where n is the normal to the insulated wall; at $t = 0$, heated wall temperature $T_w = 298$ K.

2.2 Model Validation

The numerical model is validated with the experimental work [7] where melting of lauric acid inside a rectangular enclosure was considered. A comparative study is done on the variation of melt fraction with time for the left wall temperature of 333 K as shown in Fig. 2 which shows a good agreement. The maximum error in numerical results is less than 10%. Different assumptions such as melting takes place in 2 °C temperature range and constant thermophysical property are the reason of deviation of numerical results.
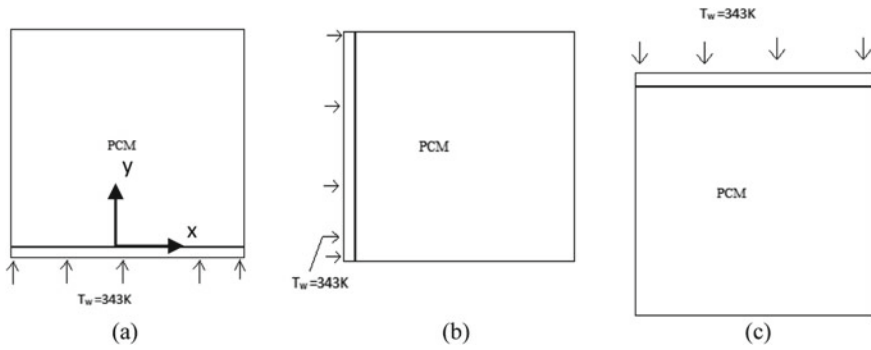
Fig. 1 Schematic of PCM enclosure under different wall heating condition (**a**) bottom wall (*case 1*) (**b**) side wall (*case 2*) (**c**) upper wall (*case 3*)

Fig. 2 Validation of numerical model
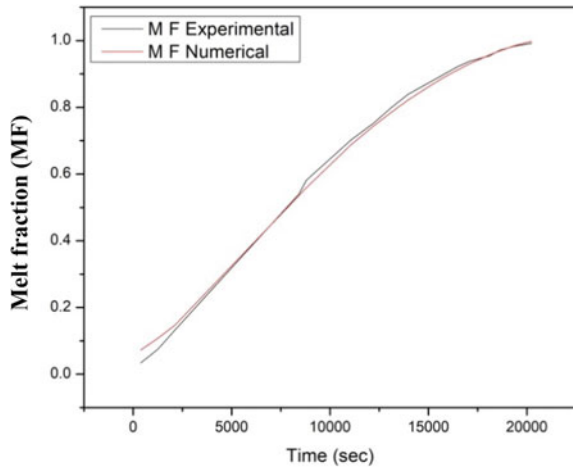
3   Results and Discussion

Figures 3 and 4 show the contour plots of melting front for all three cases at 1800s and 3600 s, respectively. It has been observed that for side wall heating the interface between liquid and solid PCM increases significantly at the later stage of melting. This increases the convective heat transfer significantly. But for the case of bottom wall, heating interface does not increase to that extent and the least rate of melting is observed for upper wall heating. The upper wall heating leads to thermal stratification as a result convective current is not generated and conduction is the only predominant mode of heat transfer for that case.

Figure 5 represents the melt fraction at different times for the considered all three cases. Heating from the side wall shows the highest melting rate among them, though at the beginning of melting process heating from bottom wall shows higher melting rate than that of heating from side wall. Because convective current encounters lesser restrictions at the beginning of convection process for bottom wall heating in comparison to side wall heating. The convective current is confined in the bottom portion of
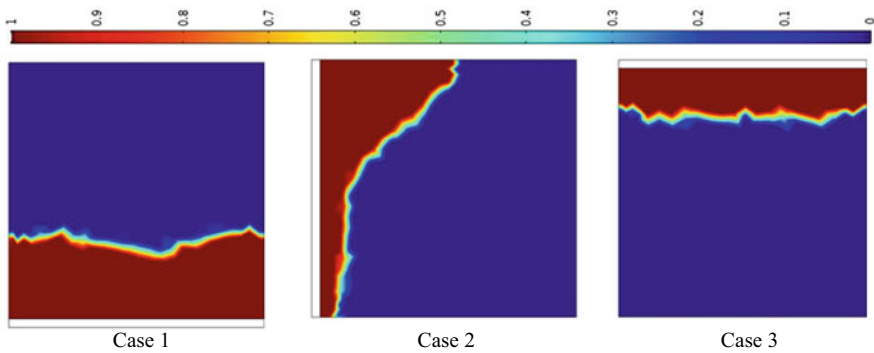

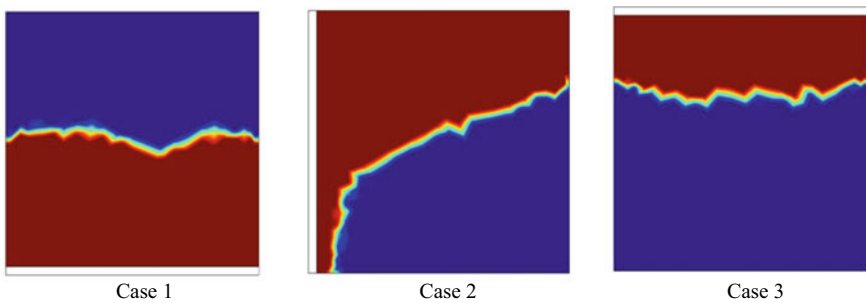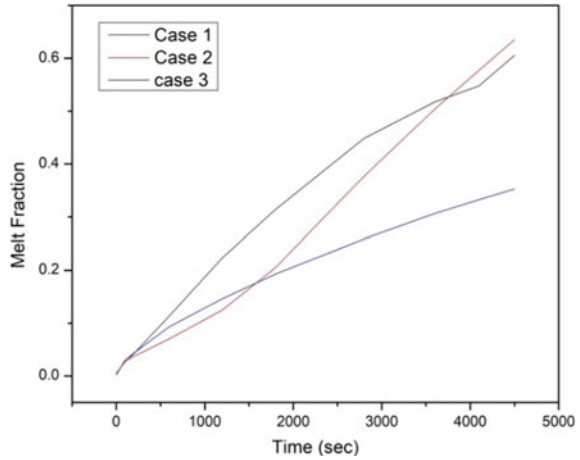**Fig. 3** Liquid fraction contour plots for all the three cases at 1800s

**Fig. 4** Liquid fraction contour plots for all the three cases at 3600 s

Fig. 5 Melt fraction
variation with time for
different heating conditions

the container for bottom wall heating. On the contrary in case of side wall heating, convective current passes through the narrow channel produced by melting of PCM.

Figure 6 represents the variation of Nusselt number (*Nu*) with time for different wall heating conditions. In the heater surface, a thin concentrated melted layer is formed in the starting phase of melting which results in a higher near wall temperature gradient. So at the beginning, *Nu* is very high. But as the thickness of the layer increases with time *Nu* decreases [9]. As time advances, the melting process is regulated by both conduction and convection process. Higher *Nu* signifies higher convective heat transfer in the melting process. For bottom wall heating, *Nu* increases up to certain time and then decreases. On the other hand, for side wall heating, *Nu* attains a very low value and then increases as time passes. But consistently lower *Nu* is observed for top wall heating case.

Fig. 6 Nusselt number
variation with time for
different heating conditions
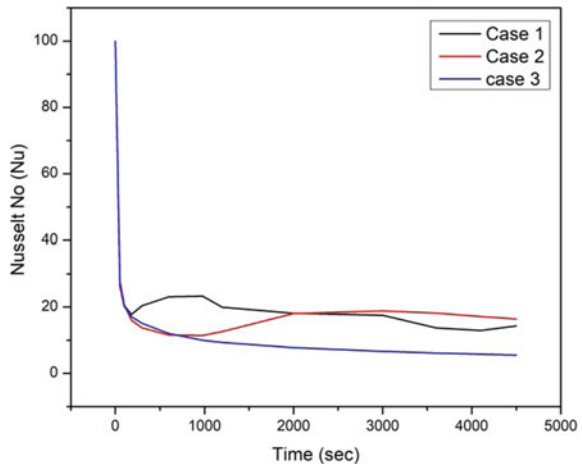
4 Conclusion

Two-dimensional analysis of PCM melting in different wall heating condition is analyzed numerically in the present study. Finite element method is used to solve the governing equations. Highest melting is observed in case of side wall heating. Though in beginning of melting process bottom wall heating gives highest melting rate, with the advancement of time, side wall melting overshoots than that of the bottom wall heating. On the other hand, top wall heating results in least melting advancement as only conduction is the predominant mode of heat transfer in this case.

References

1. B. Kamkari, H.J. Amlashi, Numerical simulation and experimental verification of constrained melting of phase change material in inclined rectangular enclosures, International Communications of. Heat Mass Transf. **88**, 211–219 (2017)
2. P.H. Biwole, D. Groulx, F. Souayfane, T. Chiu, Influence of fin size and distribution on solid-liquid phase change in a rectangular enclosure. Int. J. Therm. Sci. **124**, 433-446 (2018)
3. C. Ji, Z. Qin, Z. Low, S. Dubey, F.H. Choo, F. Duan, Non-uniform heat transfer suppression to enhance PCM melting by angled fins. Appl. Therm. Eng. **129**, 269–279 (2018)
4. A.K. Asl, S. Hossainpour, M.M. Rashidi, M.A. Sheremet, Z. Yang, Comprehensive investigation of solid and porous fins influence on natural convection in an inclined rectangular enclosure. Int. J. Heat Mass Transf. **133**, 729–744 (2019)
5. S. Ebadi, S.H. Tasnim, A.A. Aliabadi, S. Mahmud, Melting of nano-PCM inside a cylindrical thermal energy storage system: numerical study with experimental verification. Energy Conserv. Manage. **166**, 241–259 (2018)
6. S. Arena, E. Casti, J. Gasia, L.F. Cabeza, G. Cau, Numerical analysis of a latent heat thermal energy storage system under partial load operating conditions. Renew. Energy **128**, 350–361 (2018)
7. H. Shokouhmand, B. Kamkari, Experimental investigation on melting heat transfer characteristics of lauric acid in a rectangular thermal storage unit. Exp. Therm. Fluid. Sci. **50**, 201–212 (2013)
8. M. Dhar, N. Barman, S. Mandal, H. Chattopadhyay, Remelting and interface dynamics during solidification of a eutectic solution in a top-cooled rectangular cavity: a numerical study. Int. J. Heat Mass Transf. **77**, 730–737 (2014)
9. M. Alomair, Y. Alomair, S. Tasnim, S. Mahmud, H. Abdullah, Analyses of Bio-based nano-PCM filled concentric cylindrical energy storage system in vertical orientation. J. Energy Storage **20**, 380–394 (2018)